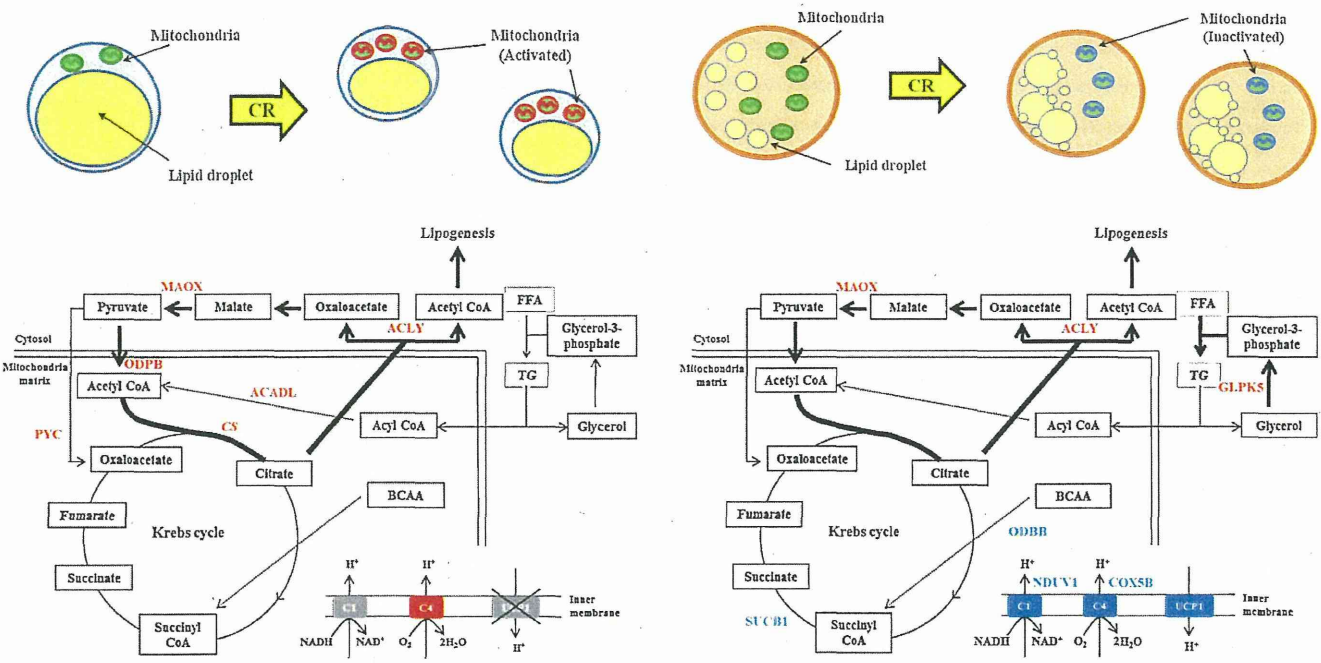

Fig. 7. Schematic diagram of the differential responses of WAT and BAT to CR based on the present study. In WAT, CR activates various mitochondrial functions including the Krebs cycle and the electron transport chain. It also accelerates fatty acid biosynthesis. It is likely that in CR rats WAT functions as an energy transducer from glucose to more energy-dense lipids and not as an energy storage system (A). In BAT, CR does not activate mitochondrial functions, but activates fatty acid biosynthesis. It is likely that in CR rats BAT functions as an energy reservoir system in the form of TG (B). CR-associated functional alterations of mitochondria significantly differ between WAT and BAT. However, it is likely that CR activates fatty acid biosynthesis and pyruvate/citrate cycling in both WAT and BAT. Expression of genes or proteins and enzymatic activities that were up-regulated by CR are indicated by red letters, and those down-regulated by CR are indicated by blue letters. *ACADL*: long-chain specific acyl-CoA dehydrogenase, mitochondrial; ACLY: ATP-citrate synthase; COX4: cytochrome c oxidase 4; COX5B: cytochrome c oxidase subunit 5B; CS: citrate synthase; FFA: free fatty acid; GLPK5: glycerol kinase 5; MAOX: NADP-dependent malic enzyme; NDUV1: NADH dehydrogenase flavoprotein 1, mitochondrial; ODBB: 2-oxoisovalerate subunit beta; ODPB: pyruvate dehydrogenase E1 component subunit beta, mitochondrial; PYC: pyruvate carboxylase, mitochondrial; SUCB1: succinyl-CoA ligase [ADP-forming] subunit beta, mitochondrial; TG: triglyceride; UCP1: uncoupling protein 1.

involved in pyruvate/malate cycling, are important regulators of lifespan in yeast (Easlon et al., 2007, 2008). Therefore, pyruvate/malate cycling may be a novel key regulator of the anti-aging and pro-longevity effects of CR.

Based on our data, we conclude that CR activates *de novo* fatty acid biosynthesis in both WAT and BAT. In contrast, CR enhances mitochondrial function in WAT but does not in BAT. The remodeling of both WAT and BAT, which is characterized by effective energy utilization, may promote beneficial actions associated with CR.

Acknowledgements

We thank all members of the Molecular Pathology and Metabolic Disease and Animal Center of Faculty of Pharmaceutical Sciences, Tokyo University of Science, for their cooperation. We also thank Professor Isao Shimokawa, Yutaka Araki and Yuko Moriyama in the Department of Investigative Pathology, Nagasaki University Graduate School of Biomedical Sciences, for their invaluable technical assistance. This work was partially supported by a Grant-in-Aid for Scientific Research (C) from the Japan Society for the Promotion of Science (19590396) and a Grant-in-Aid for the Third-term Comprehensive 10-year Strategy for Cancer Control from the Ministry of Health, Labor and Welfare, Japan.

References

Alp, P.R., Newsholme, E.A., Zammit, V.A., 1976. Activities of citrate synthase and NAD+-linked and NADP+-linked isocitrate dehydrogenase in muscle from vertebrates and invertebrates. Biochem. J. 154, 689–700.

Anderson, R., Prolla, T., 2009. PGC-1alpha in aging and anti-aging interventions. Biochim. Biophys. Acta 1790, 1059–1066.

Argmann, C., Dobrin, R., Heikkinen, S., Auburtin, A., Pouilly, L., Cock, T.A., Koutnikova, H., Zhu, J., Schadt, E.E., Auwerx, J., 2009. Ppargamma2 is a key driver of longevity in the mouse. PLoS Genet. 5, e1000752.

Balwierz, A., Polus, A., Razny, U., Wator, L., Dyduch, G., Tomaszewska, R., Scherneck, S., Joost, H., Dembinska-Kiec, A., 2009. Angiogenesis in the New Zealand obese mouse model fed with high fat diet. Lipids Health Dis. 8, 13.

Barzilai, N., Banerjee, S., Hawkins, M., Chen, W., Rossetti, L., 1998. Caloric restriction reverses hepatic insulin resistance in aging rats by decreasing visceral fat. J. Clin. Invest. 101, 1353–1361.

Berwick, D.C., Hers, I., Heesom, K.J., Moule, S.K., Tavare, J.M., 2002. The identification of ATP-citrate lyase as a protein kinase B (AKT) substrate in primary adipocytes. J. Biol. Chem. 277, 33895–33900.

Blüher, M., Michael, M.D., Peroni, O.D., Ueki, K., Carter, N., Kahn, B.B., Kahn, C.R., 2002. Adipose tissue selective insulin receptor knockout protects against obesity and obesity-related glucose intolerance. Dev. Cell 3, 25–38.

Blüher, M., Kahn, B.B., Kahn, C.R., 2003. Extended longevity in mice lacking the insulin receptor in adipose tissue. Science 299, 572–574.

Capaldi, R.A., 1990. Structure and assembly of cytochrome c oxidase. Arch. Biochem. Biophys. 280, 252–262.

Chiu, C.H., Lin, W.D., Huang, S.Y., Lee, Y.H., 2004. Effect of a C/EBP gene replacement on mitochondrial biogenesis in fat cells. Genes Dev. 18, 1970–1975.

Colman, R.J., Anderson, R.M., Johnson, S.C., Kastman, E.K., Kosmatka, K.J., Beasley, T.M., Allison, D.B., Cruzen, C., Simmons, H.A., Kemnitz, J.W., Weindruch, R., 2009. Caloric restriction delays disease onset and mortality in rhesus monkeys. Science 325, 201–204.

Daley, E., Wilkie, D., Loesch, A., Hargreaves, I.P., Kendall, D.A., Pilkington, G.J., Bates, T.E., 2005. Chlorimipramine: a novel anticancer agent with a mitochondrial target. Biochem. Biophys. Res. Commun. 328, 623–632.

DeClercq, V., Taylor, C., Zahradka, P., 2008. Adipose tissue: the link between obesity and cardiovascular disease. Cardiovasc. Hematol. Disord. Drug Targets 8, 228–237.

Dosh, B.M., Hightower, L.E., Lee, J., 2010. HSPB1, actin filament dynamics, and aging cells. Ann. N.Y. Acad. Sci. 1197, 76–84.

Dumas, J.F., Roussel, D., Simard, G., Douay, O., Foussard, F., Malthiery, Y., Ritz, P., 2004. Food restriction affects energy metabolism in rat liver mitochondria. Biochim. Biophys. Acta 1670, 126–131.

Easlon, E., Tsang, F., Dilova, I., Wang, C., Lu, S.P., Skinner, C., Lin, S.J., 2007. The dihydrolipoamide acetyltransferase is a novel metabolic longevity factor and is required for calorie restriction-mediated life span extension. J. Biol. Chem. 282, 6161–6171.

Easlon, E., Tsang, F., Skinner, C., Wang, C., Lin, S.J., 2008. The malate-aspartate NADH shuttle components are novel metabolic longevity regulators required for calorie restriction-mediated life span extension in yeast. Genes Dev. 22, 931–944.
Farmer, S.R., 2006. Transcriptional control of adipocyte formation. Cell Metab. 4, 263–273.
Farmer, S.R., 2008. Molecular determinants of brown adipocyte formation and function. Genes Dev. 22, 1269–1275.
Frayn, K.N., 2002. Adipose tissue as a buffer for daily lipid flux. Diabetologia 45, 1201–1210.
Gnacińska, M., Małgorzewicz, S., Stojek, M., Łysiak-Szydłowska, W., Sworczak, K., 2009. Role of adipokines in complications related to obesity: a review. Adv. Med. Sci. 54, 150–157.
Griffin, M.J., Sul, H.S., 2004. Insulin regulation of fatty acid synthase gene transcription: roles of USF and SREBP-1c. IUBMB Life 56, 595–600.
Guay, C., Madiraju, S.R., Aumais, A., Joly, E., Prentki, M., 2007. A role for ATP-citrate lyase, malic enzyme, and pyruvate/citrate cycling in glucose-induced insulin secretion. J. Biol. Chem. 282, 35657–35665.
Higami, Y., Pugh, T.D., Page, G.P., Allison, D.B., Prolla, T.A., Weindruch, R., 2004. Adipose tissue energy metabolism: altered gene expression profile of mice subjected to long-term caloric restriction. FASEB J. 18, 415–417.
Higami, Y., Yamaza, H., Shimokawa, I., 2005. Laboratory findings of caloric restriction in rodents and primates. Adv. Clin. Chem. 39, 211–237.
Higami, Y., Barger, J.L., Page, G.P., Allison, D.B., Smith, S.R., Prolla, T.A., Weindruch, R., 2006a. Energy restriction lowers the expression of genes linked to inflammation, the cytoskeleton, the extracellular matrix, and angiogenesis in mouse adipose tissue. J. Nutr. 136, 343–352.
Higami, Y., Tsuchiya, T., Chiba, T., Yamaza, H., Muraoka, I., Hirose, M., Komatsu, T., Shimokawa, I., 2006b. Hepatic gene expression profile of lipid metabolism in rats: Impact of caloric restriction and growth hormone/insulin-like growth factor-1 suppression. J. Gerontol. A: Biol. Sci. Med. Sci. 61, 1099–1110.
Hotamisligil, G.S., Arner, P., Caro, J.F., Atkinson, R.L., Spiegelman, B.M., 1995. Increased adipose tissue expression of tumor necrosis factor-alpha in human obesity and insulin resistance. J. Clin. Invest. 95, 2409–2415.
Huh, T.L., Casazza, J.P., Huh, J.W., Chi, Y.T., Song, B.J., 1990. Characterization of two cDNA clones for pyruvate dehydrogenase E1 beta subunit and its regulation in tricarboxylic acid cycle-deficient fibroblast. J. Biol. Chem. 265, 13320–13326.
Ikeda, Y., Okamura-Ikeda, K., Tanaka, K., 1985. Purification and characterization of short-chain, medium-chain, and long-chain acyl-CoA dehydrogenases from rat liver mitochondria. Isolation of the holo- and apoenzymes and conversion of the apoenzyme to the holoenzyme. J. Biol. Chem. 260, 1311–1325.
Ikegami, K., Setou, M., 2009. TTLL10 can perform tubulin glycylation when co-expressed with TTLL8. FEBS Lett. 583, 1957–1963.
Jahnke, V.E., Sabido, O., Defour, A., Castells, J., Lefai, E., Roussel, D., Freyssenet, D., 2010. Evidence for mitochondrial respiratory deficiency in rat rhabdomyosarcoma cells. PLoS One 5, e8637.
Jensen, M.V., Joseph, J.W., Ronnebaum, S.M., Burgess, S.C., Sherry, A.D., Newgard, C.B., 2008. Metabolic cycling in control of glucose-stimulated insulin secretion. Am. J. Physiol. Endocrinol. Metab. 295, E1287–E1297.
Jitrapakdee, S., Vidal-Puig, A., Wallace, J.C., 2006. Anaplerotic roles of pyruvate carboxylase in mammalian tissues. Cell. Mol. Life Sci. 63, 843–854.
Kang, D., Kim, S.H., Hamasaki, N., 2007. Mitochondrial transcription factor A (TFAM): roles in maintenance of mtDNA and cellular functions. Mitochondrion 7, 39–44.
Katic, M., Kennedy, A.R., Leykin, I., Norris, A., McGettrick, A., Gesta, S., Russell, S.J., Bluher, M., Maratos-Flier, E., Kahn, C.R., 2007. Mitochondrial gene expression and increased oxidative metabolism: role in increased lifespan of fat-specific insulin receptor knock-out mice. Aging Cell 6, 827–839.
Kenyon, C., 2005. The plasticity of aging: insights from long-lived mutants. Cell 120, 449–460.
Kerscher, S., Dröse, S., Zickermann, V., Brandt, U., 2008. The three families of respiratory NADH dehydrogenases. Results Probl. Cell Differ. 45, 185–222.
Koekemoer, T.C., Downing, T.G., Oelofsen, W., 1998. An alternative PCR assay for quantifying mitochondrial DNA in crude preparations. Nucleic Acids Res. 26, 2829–2830.
Lambeth, D.O., Tews, K.N., Adkins, S., Frohlich, D., Milavetz, B.I., 2004. Expression of two succinyl-CoA synthetases with different nucleotide specificities in mammalian tissues. J. Biol. Chem. 279, 36621–36624.
Lenka, N., Vijayasarathy, C., Mullick, J., Avadhani, N.G., 1998. Structural organization and transcription regulation of nuclear genes encoding the mammalian cytochrome c oxidase complex. Prog. Nucleic Acid Res. Mol. Biol. 61, 309–344.
Liang, H., Ward, W.F., 2006. PGC-1alpha: a key regulator of energy metabolism. Adv. Physiol. Educ. 30, 145–151.
Masoro, E.J., 2005. Overview of caloric restriction and ageing. Mech. Ageing Dev. 126, 913–922.
Nakamura, M., Yamada, M., Ohsawa, T., Morisawa, H., Nishine, T., Nishimura, O., Toda, T., 2006. Phosphoproteomic profiling of human SH-SY5Y neuroblastoma cells during response to 6-hydroxydopamine-induced oxidative stress. Biochim. Biophys. Acta 1763, 977–989.
Nisoli, E., Tonello, C., Cardile, A., Cozzi, V., Bracale, R., Tedesco, L., Falcone, S., Valerio, A., Cantoni, O., Clementi, E., Moncada, S., Carruba, M.O., 2005. Calorie restriction promotes mitochondrial biogenesis by inducing the expression of eNOS. Science 310, 314–317.
Otabe, S., Yuan, X., Fukutani, T., Wada, N., Hashinaga, T., Nakayama, H., Hirota, N., Kojima, M., Yamada, K., 2007. Overexpression of human adiponectin in transgenic mice results in suppression of fat accumulation and prevention of premature death by high-calorie diet. Am. J. Physiol. Endocrinol. Metab. 293, E210–E218.
Puigserver, P., Spiegelman, B.M., 2003. Peroxisome proliferator-activated receptor-gamma coactivator 1 alpha (PGC-1 alpha): transcriptional coactivator and metabolic regulator. Endocr. Rev. 24, 78–90.
Ramakrishna, S., Benjamin, W.B., 1979. Fat cell protein phosphorylation. Identification of phosphoprotein-2 as ATP-citrate lyase. J. Biol. Chem. 254, 9232–9236.
Saely, C.H., Geiger, K., Drexel, H., 2010. Brown versus white adipose tissue: a mini-review. Gerontology [Epub ahead of print].
Sakai, T., Sakaue, H., Nakamura, T., Okada, M., Matsuki, Y., Watanabe, E., Hiramatsu, R., Nakayama, K., Nakayama, K.I., Kasuga, M., 2007. Skp2 controls adipocyte proliferation during the development of obesity. J. Biol. Chem. 282, 2038–2046.
Salway, T.G., 1999. Metabolism at a Glance, 2nd ed. Blackwell Science Ltd., Oxford, UK.
She, P., Van Horn, C., Reid, T., Hutson, S.M., Cooney, R.N., Lynch, C.J., 2007. Obesity-related elevations in plasma leucine are associated with alterations in enzymes involved in branched-chain amino acid metabolism. Am. J. Physiol. Endocrinol. Metab. 293, E1552–E1563.
Shi, T., Wang, F., Stieren, E., Tong, Q., 2005. SIRT3, a mitochondrial sirtuin deacetylase, regulates mitochondrial function and thermogenesis in brown adipocytes. J. Biol. Chem. 280, 13560–13567.
Sinclair, D.A., 2005. Toward a unified theory of caloric restriction and longevity regulation. Mech. Ageing Dev. 126, 987–1002.
Stofkova, A., 2009. Leptin and adiponectin: from energy and metabolic dysbalance to inflammation and autoimmunity. Endocr. Regul. 43, 157–168.
Sugden, M.C., Holness, M.J., 2003. Recent advances in mechanisms regulating glucose oxidation at the level of the pyruvate dehydrogenase complex by PDKs. Am. J. Physiol. Endocrinol. Metab. 284, E855–E862.
Taroni, F., Di Donato, S., 1988. Purification and properties of cytosolic malic enzyme from human skeletal muscle. Int. J. Biochem. 20, 857–866.
Torres-Leal, F.L., Fonseca-Alaniz, M.H., Rogero, M.M., Tirapegui, J., 2010. The role of inflamed adipose tissue in the insulin resistance. Cell Biochem. Funct. 28, 623–631.
Valle, A., Sastre-Serra, J., Roca, P., Oliver, J., 2010. Modulation of white adipose tissue proteome by aging and calorie restriction. Aging Cell 9, 882–894.
Wang, X., Paigen, B., 2005. Genetics of variation in HDL cholesterol in humans and mice. Circ. Res. 96, 27–42.
Watford, M., 2000. Functional glycerol kinase activity and the possibility of a major role for glyceroneogenesis in mammalian skeletal muscle. Nutr. Rev. 58, 145–148.
Weindruch, R., Walford, R.L., 1988. The Retardation of Aging and Disease by Dietary Restriction. Charles C Thomas Publisher, Springfield, IL.
Wiegand, G., Remington, S.J., 1986. Citrate synthase: structure control, and mechanism. Annu. Rev. Biophys. Biophys. Chem. 15, 97–117.
Yamauchi, T., Kamon, J., Waki, H., Terauchi, Y., Kubota, N., Hara, K., Mori, Y., Ide, T., Murakami, K., Tsuboyama-Kasaoka, N., Ezaki, O., Akanuma, Y., Gavrilova, O., Vinson, C., Reitman, M.L., Kagechika, H., Shudo, K., Yoda, M., Nakano, Y., Tobe, K., Nagai, R., Kimura, S., Tomita, M., Froguel, P., Kadowaki, T., 2001. The fat-derived hormone adiponectin reverses insulin resistance associated with both lipoatrophy and obesity. Nat. Med. 7, 941–946.
Yamauchi, T., Kamon, J., Minokoshi, Y., Ito, Y., Waki, H., Uchida, S., Yamashita, S., Noda, M., Kita, S., Ueki, K., Eto, K., Akanuma, Y., Froguel, P., Foufelle, F., Ferre, P., Carling, D., Kimura, S., Nagai, R., Kahn, B.B., Kadowaki, T., 2002. Adiponectin stimulates glucose utilization and fatty-acid oxidation by activating AMP-activated protein kinase. Nat. Med. 8, 1288–1295.
Yamaza, H., Komatsu, T., To, K., Toyama, H., Chiba, T., Higami, Y., Shimokawa, I., 2007. Involvement of insulin-like growth factor-1 in the effect of caloric restriction: regulation of plasma adiponectin and leptin. J. Gerontol. A: Biol. Sci. Med. Sci. 62, 27–33.
Yu, B.P., 1994. Modulation of Aging Processes by Dietary Restriction. CRC Press, Boca Raton, FL.
Zhu, M., Lee, G.D., Ding, L., Hu, J., Qiu, G., de Cabo, R., Bernier, M., Ingram, D.K., Zou, S., 2007. Adipogenic signaling in rat white adipose tissue: modulation by aging and calorie restriction. Exp. Gerontol. 42, 733–744.

Biochemical and Biophysical Research Communications 427 (2012) 758–763

Contents lists available at SciVerse ScienceDirect

Biochemical and Biophysical Research Communications

journal homepage: www.elsevier.com/locate/ybbrc

Autophagosomes accumulate in differentiated and hypertrophic adipocytes in a p53-independent manner

Kentaro Mikami, Naoyuki Okita, Yuki Tokunaga, Tomoyo Ichikawa, Tatsuya Okazaki, Kanako Takemoto, Wataru Nagai, Shingo Matsushima, Yoshikazu Higami *

Molecular Pathology & Metabolic Disease, Faculty of Pharmaceutical Sciences, Tokyo University of Science, Tokyo, Japan

ARTICLE INFO

Article history:
Received 25 September 2012
Available online 4 October 2012

Keywords:
p53
Adipocyte
Differentiation
Obesity
Autophagosome
Autophagic flux

ABSTRACT

Autophagy is induced by several kinds of stress, including oxidative, genotoxic, endoplasmic reticulum and nutrient stresses. The tumor suppressor p53, which is a stress sensor, plays a critical role in the regulation of autophagy. Although p53 is required for starvation (nutrient deficient stress)-induced autophagy, it is still not clear whether p53 is also required for the autophagy observed in differentiated and hypertrophic adipocytes, which accumulate excessive amounts of nutrients in the form of triglycerides. In this study, we demonstrated that starvation induces autophagy in p53-proficient adipocytes, but not in p53-deficient adipocytes as previously reported. On the other hand, autophagy was equally observed in both p53-deficient and -proficient differentiated and hypertrophic adipocytes. Similar results were obtained by *in vivo* analysis using white adipose tissue of high-fat diet-induced obese mice. Moreover, unexpectedly, the autophagy observed in the differentiated and hypertrophic adipocytes involved increased accumulation of autophagosomes and decreased autophagic flux. Thus, we concluded that in differentiated and hypertrophic adipocytes autophagosomes accumulate in a p53-independent manner, and this accumulation is caused by reduced autophagic flux.

1. Introduction

Autophagy is a major cytosolic catabolic process operating through the lysosomal machinery, and playing an important role in cellular and/or organism homeostasis against diverse pathologies [1–4]. In this process, autophagy is initiated by autophagosome formation, surrounding cytoplasmic components with a double-membrane. Then, the autophagosome fuses with a lysosome to form an autolysosome and subsequently degrades the intramembrane contents. During autophagosome formation, microtubule-associated protein 1–light chain 3 (LC3) is lipidated, converting LC3-I (non-lipidated form) to LC3-II (lipidated form). Autophagy is the key machinery for the turnover of cellular components and/or proteins including p62, which seems to be a selective substrate for autophagy [2–4]. Therefore, the conversion of LC3-I to LC3-II, the aggregation of LC3-II and the degradation of p62 are hallmarks of the autophagic process [2–4].

The tumor suppressor p53 is involved in several cellular stress responses [5]. Recently, it has been reported that p53 plays a critical role in the autophagic process and metabolic process [6–10]. p53 promotes autophagy through inhibition of mammalian target of rapamycin (mTOR) [8]. p53 also transcriptionally promotes the expression of autophagy-regulated genes such as Sestrin2 and DRAM [9,10].

Previously, it has been reported that autophagic vacuoles are frequently found in differentiated and hypertrophic 3T3-L1 adipocytes [11]. Furthermore, targeted deletion of atg5 or atg7, which are necessary for the autophagic process, interferes with normal adipocyte differentiation, suggesting that autophagy regulates adipocyte differentiation and/or lipid accumulation [12–15]. Moreover, inhibition of autophagy increases triglyceride storage in lipid droplets in cultured hepatocytes and mouse liver [16]. Thus, these studies indicate that autophagy is involved in adipogenesis and lipid metabolism.

In the present study, to understand the molecular basis of autophagy observed in differentiated and hypertrophic adipocytes, we investigated whether p53 is required for autophagy in differentiated and hypertrophic adipocytes associated with excessive nutrient accumulation using both *in vitro* and *in vivo* models. Moreover, we evaluated whether the autophagic machinery is fully activated in differentiated and hypertrophic adipocytes *in vitro*.

2. Materials and methods

2.1. Animals

Experiments on mice were conducted in accordance with the provisions of the Ethics Review Committee for Animal

* Corresponding author. Address: Molecular Pathology & Metabolic Disease, Faculty of Pharmaceutical Sciences, Tokyo University of Science, 2641 Yamazaki, Noda, Chiba 278-8510, Japan. Fax: +81 4 7121 3676.
E-mail address: higami@rs.noda.tus.ac.jp (Y. Higami).

0006-291X/$ - see front matter © 2012 Elsevier Inc. All rights reserved.
http://dx.doi.org/10.1016/j.bbrc.2012.09.134

Experimentation at Tokyo University of Science. p53 heterozygous knockout ($p53^{+/-}$) mice with C57BL/6J background (Accession Number, CDB0001K) were purchased from RIKENBRC (Saitama, Japan). These mice were intercrossed to obtain wild-type ($p53^{+/+}$) and homozygous knockout ($p53^{-/-}$) mice. Male $p53^{+/+}$ and $p53^{-/-}$ mice were weaned four weeks after birth. Mice were housed in a temperature-controlled environment with a 12-h light/dark cycle and free access to water and a normal-fat diet (NFD; NOSAN, Kanagawa, Japan) or high-fat diet (HFD; CREA, Tokyo, Japan) for nine weeks. Mice were sacrificed at 13 weeks of age and the epididymal white adipose tissue (WAT) was collected.

2.2. Cell lines and reagents

The p53-proficient preadipocyte cell line, 3T3-L1, was purchased from RIKENBRC. The p53-deficient preadipocyte cell line, HW, was kindly provided by Dr. Masayuki Saito (Tenshi University, Japan). Primary mouse embryonic fibroblasts (MEFs) derived from wildtype ($p53^{+/+}$) and p53-knockout ($p53^{-/-}$) mice were established as previously described [17].

Etoposide and camptothecin were purchased from WAKO (Osaka, Japan). Rapamycin and bafilomycin A1 were purchased from LC Laboratories (Woburn, MA, USA).

2.3. Vector construction

The pMXs-puro (-U3) –Cul2 and pMXs-puro (-U3) Kpc1 vectors were kindly gifted by Dr. Takumi Kamura (Nagoya University, Japan). To construct the backbone vector, pMXs-puro-mU6 [18], the mouse U6 gene promoter was obtained from the pMXs-puro (-U3) Kpc1 vector by PCR, using the following primers: forward – 5′-GGCAAAACTCGAGTTCGAACGCGTGATCAATTGTTTAAACAAGGCT TTTCTCCAGGGATATTTATAGTA-3′, and reverse – 5′-GTCGAC-CACTGTGCTGGC-3′. The PCR product was digested with NotI/XhoI and subcloned into the NotI/XhoI sites of the pMXs-puro (-U3) – Cul2 vector, yielding the pMXs-puro-mU6 shRNA vector. We designed a mouse p53 shRNA expression vector based on target sequences for effective p53 knockdown as previously reported [19]. The oligonucleotides for shp53 and the shGFP control were chemically synthesized (Operon Biotechnology, Tokyo, Japan) as follows. shp53-1: 5′-GTACGTGTGTAGTAGCTTCttcaagagaGGAGC-TATTACACATGTACttttt-3′ and 5′-cgaaaaaGTACATGTGTAATAGCTCC tctcttgaaGAAGCTACTACACACGTAC-3′; shp53-2: 5′-GGAGTAGGTT GGTAGTTGTTATTCAAGAGATGACAACTATCAACCTATTCCCCttttt-3′ and 5′-cgaaaaaGGGGAATAGGTTGATAGTTGTCATCTCTTGAATA ACAACTACCAACCTACTCC-3′; shGFP: 5′-GGCTATGTCCAGGGGCG-CATCttcaagagaGGTGCGCTCCTGGACGTAGCCttttt-3′ and 5′-cgaaaaa GGCTACGTCCAGGAGCGCACCtctcttgaaGATGCGCCCCTGGACATAGC C-3′ (upper case letters, target sequences against p53 or GFP; lower case letters, BstBI or loop structure sequences). The annealed oligos were directly ligated into a PmeI and BstBI-digested pMXs-puro-mU6 shRNA expression vector.

2.4. Establishment of stable p53-knockdown 3T3-L1 preadipocytes

Stable p53-knockdown cell lines were generated using retroviral infection as previously reported [20]. The produced vectors, termed pMXs-puro-mU6-shp53 or shGFP, were transfected into Plat-E cells with FuGENE®6 (Promega, Madison, WI, USA), according to the manufacturer's protocol. Virus-containing culture supernatants were collected 2 d after the transfection and filtered through 0.22-μm filters (Millipore, Billerica, MA, USA). To obtain stable p53- or GFP-knockdown cell lines (3T3-L1/shp53 or 3T3-L1/shGFP), 3T3-L1 cells were incubated with virus-containing medium for 2 d, followed by selection with 2 μg/mL puromycin for 5 d.

2.5. Cell culture and treatments

Preadipocyte cell lines were maintained in maintenance medium. Preadipocyte cell lines were differentiated as previously described [21]. In brief, cells were seeded to reach confluency after 2 d. At confluence, the maintenance medium was changed to adipocyte differentiation medium (AD medium), and the cells were cultured for another 2 d. For adipocyte maturation, the differentiation-induced cells were grown in adipocyte maturation medium (AM medium), which was changed every other day. The maintenance medium contained 10% FBS (Sigma, Saint Louis, MO, USA) and 1% penicillin/streptomycin (Sigma) in DMEM low glucose (WAKO). AD medium contained 500 μM 3-isobutyl-1-methylxanthine (Sigma) and 1 μM dexamethasone (Sigma) in maintenance medium, and AM medium contained 10 μg/mL insulin (Sigma) and 50 nM tri-iode thyronine (T3; Sigma) in maintenance medium.

To induce adipocyte differentiation in MEFs, MEFs were seeded to reach confluence. At confluence, the maintenance medium was changed to MEF differentiation medium, which contained 500 μM 3-isobutyl-1-methylxanthine, 1 μM dexamethasone, 10 μg/mL insulin and 100 μM troglitazone (WAKO). The medium was changed to fresh MEF differentiation medium every other day.

To induce nutrient starvation, the maintenance medium was changed to DMEM without FBS (serum-free) followed by incubation for 24 h. To induce autophagy via inhibition of mTOR, cells were treated with 500 nM rapamycin for 6 h.

To analyze autophagic flux, adipocytes were differentiated for 3 or 11 d, followed by a medium change with fresh AM medium containing 10 nM bafilomycin A1 (Baf; LC Laboratories) for a 24-h incubation.

2.6. Western blot

Western blot analysis was performed as previously described [17] with the following primary antibodies: LC3 (PM036, MBL, Nagoya, Japan), p62 (PM045, MBL), p53 (PO03, MBL), β-actin (A1978, Sigma) and α-tubulin (T6199, Calbiochem, Darmstadt, Germany). The secondary antibodies used were: horseradish peroxidase-conjugated $F(ab')_2$ fragment of goat anti-mouse IgG or anti-rabbit IgG (Jackson Immunoresearch, West Grove, PA, USA).

2.7. Oil Red O staining

Cells were fixed with 10% neutral-buffered formalin. Fixed cells were washed with 60% isopropanol and stained with 60% isopropanol containing 0.18% Oil Red O for 20 min. Stained cells were washed with 60% isopropanol for 1 min. Images were captured by a BIOREVO BZ9000 fluorescence microscope (KEYENCE, Osaka, Japan).

2.8. Immunocytochemistry and confocal laser microscopy

Cells were seeded on poly-D-lysine-coated coverslips. For LC3 immunocytochemistry, cells were fixed in 4% paraformaldehyde and permeabilized with PBS containing 0.2% Triton-X 100 for 10 min. After washing with PBS containing 0.1% Tween 20 (TPBS), cells were blocked in TPBS containing 2% BSA and 5% goat serum. Following washes with TPBS, cells were incubated with LC3 antibodies in a moist chamber overnight at 4 °C. Next, cells were washed with TPBS and probed with the secondary antibody, Alexa Fluor 488-conjugated $F(ab')_2$ fragment of goat anti-rabbit IgG (Invitrogen, Carlsbad, CA, USA), for 30 min at room temperature. Confocal fluorescence images were captured using an LSM5Pascal Exciter laser-scanning microscope (Zeiss, Oberkochen, Germany).

2.9. Transmission electron microscopy analysis

Differentiated adipocytes were fixed with 2.5% gluteraldehyde in 0.2 M cacodylate buffer for 60 min, followed by incubation with 1% osmium tetroxide for 30 min. The samples were embedded in Epon. Selected areas were then sectioned with a Sorvall ultramicrotome MT-2 (Leica Mikrosystem GmbH, Vienna, Austria). Sections were observed under a JEM 1200EX II electron microscope (JEOL LTD, Tokyo, Japan) at 90 kV accelerating voltage.

2.10. Statistical analysis

Statistical analysis was performed by Tukey–Kramer test or Student's *t*-test (comparison of two means). The data are presented as mean ± standard deviation (S.D.). A *p*-value of less than 0.05 was considered significant.

3. Results

3.1. p53 is required for starvation-induced autophagy in 3T3-L1 and HW adipocytes

Treatment with the topoisomerase II inhibitor, etoposide, activated p53 in 3T3-L1 ($p53^{+/+}$) preadipocytes, but not in HW ($p53^{-/-}$) preadipocytes (Fig. 1A). mTOR plays a central role in the regulation of autophagy, and rapamycin induces autophagy via inhibition of mTOR [22]. In both 3T3-L1 and HW cells, 4 d after the induction of differentiation (day 4 adipocytes) rapamycin induced the conversion of LC3-I to LC3-II (Fig. 1B and C). In contrast, nutrient starvation (serum-free) induced the LC3 conversion and p62 degradation in day 4 3T3-L1 adipocytes, but not in day 4 HW adipocytes (Fig. 1D and E). Using confocal fluorescence microscopy analysis we observed that rapamycin treatment markedly increased LC3-positive puncta in both day 4 3T3-L1 and HW adipocytes. In contrast, after nutrient starvation LC3-positive puncta were increased in 3T3-L1 adipocytes but not in HW adipocytes (Fig. 1F). In agreement with previous reports [9,23], these findings suggest that p53 is necessary for starvation-induced autophagy in adipocytes.

3.2. p53 does not influence autophagy observed in differentiated and hypertrophic adipocytes

Oil Red O staining showed that 3T3-L1 and HW adipocytes accumulated TG (triglyceride) during adipocyte differentiation (Fig. 2A). Next, we investigated whether p53 participates in autophagy found at the late stage of adipocyte differentiation. The expression level of LC3-II in day 4 3T3-L1 and HW adipocytes was markedly suppressed compared with 3T3-L1 and HW preadipocytes, probably due to the medium change to insulin and tri-iode thyronine (T3) containing medium. The expression level of LC3-II in both 3T3-L1 and HW cells was similarly and significantly increased at the late stage of adipocyte differentiation (day 12 hypertrophic adipocytes) compared with day 4 adipocytes (Fig. 2B and C). In addition, LC3-positive puncta were found in both day 12 hypertrophic 3T3-L1 and HW adipocytes (Fig. 2D). Using electron microscopy several autophagosomes were observed in both day 12 hypertrophic adipocytes (Fig. 2E). These findings suggest that autophagy might be activated in differentiated and hypertrophic adipocytes in a p53-independent manner.

To confirm that the autophagy found in differentiated and hypertrophic adipocytes is p53-independent, we established stable shp53 3T3-L1 preadipocytes (3T3-L1/shp53). In 3T3-L1/shp53 preadipocytes, the camptothecin-induced p53 activation was markedly suppressed compared with 3T3-L1/shGFP preadipocytes (Fig. 3A). The expression of LC3-II and p62 was similarly increased during adipocyte differentiation in both 3T3-L1/shGFP and 3T3-L1/shp53 adipocytes (Fig. 3B). To further examine whether the autophagy observed in differentiated and hypertrophic adipocytes is p53-independent, primary mouse embryonic fibroblasts (MEFs) derived from wild type ($p53^{+/+}$) and p53-knockout ($p53^{-/-}$) mice were established. Oil Red O staining showed that both MEFs accumulated TG similarly after the induction of adipocyte differentiation for 20 d (Fig. 3C). Furthermore, the conversion of LC3-I to LC3-II was equally enhanced with the increased TG accumulation (Fig. 3D). These findings suggest that p53 does not influence the autophagic machinery observed in differentiated and hypertrophic adipocytes.

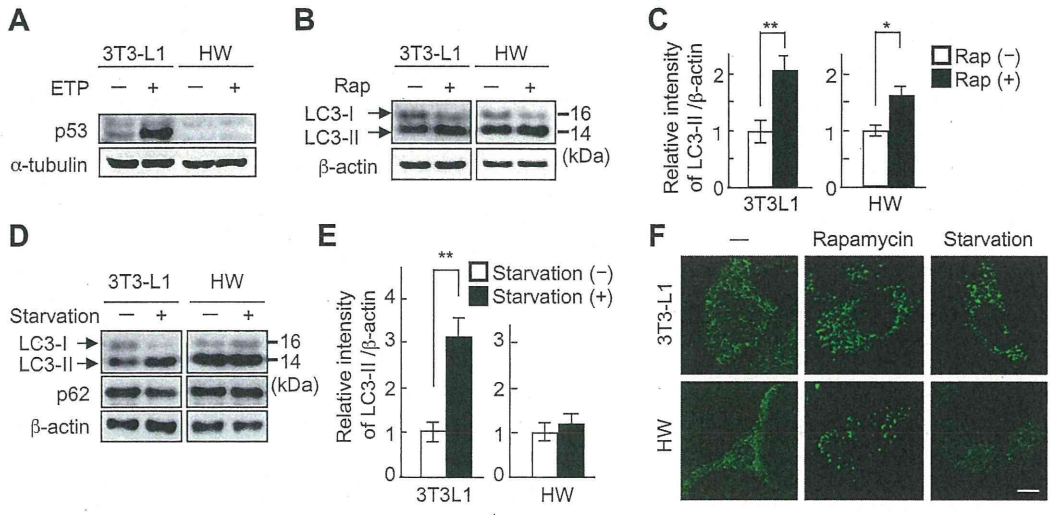

Fig. 1. p53 is required for starvation-induced autophagy. (A) 3T3-L1 and HW preadipocytes were treated with 100 μM etoposide (ETP) for 24 h. Cells were lysed and immunoblot analysis was performed using anti-p53 and anti-α-tubulin antibodies. α-Tubulin was used as a loading control. (B–E) 3T3-L1 and HW adipocytes (day 4 adipocytes) were treated with 500 nM rapamycin (Rap) for 6 h (B, C) or serum-free medium (Starvation) for 24 h (D, E). Cells were lysed and immunoblot analysis was performed with anti-LC3, anti-p62 and anti-β-actin antibodies. β-Actin was used as a loading control. The results are expressed as the relative intensity of LC3-II/β-actin compared with control cells. Values are mean ± S.D. (experiments were performed in duplicate with three independent cultures per experiment). Differences between values were analyzed by Student's *t*-test. $^{*}p < 0.05$, $^{**}p < 0.01$. (F) Immunofluorescence analysis of LC3 was performed on day 4 adipocytes. Scale bar 20 μm.

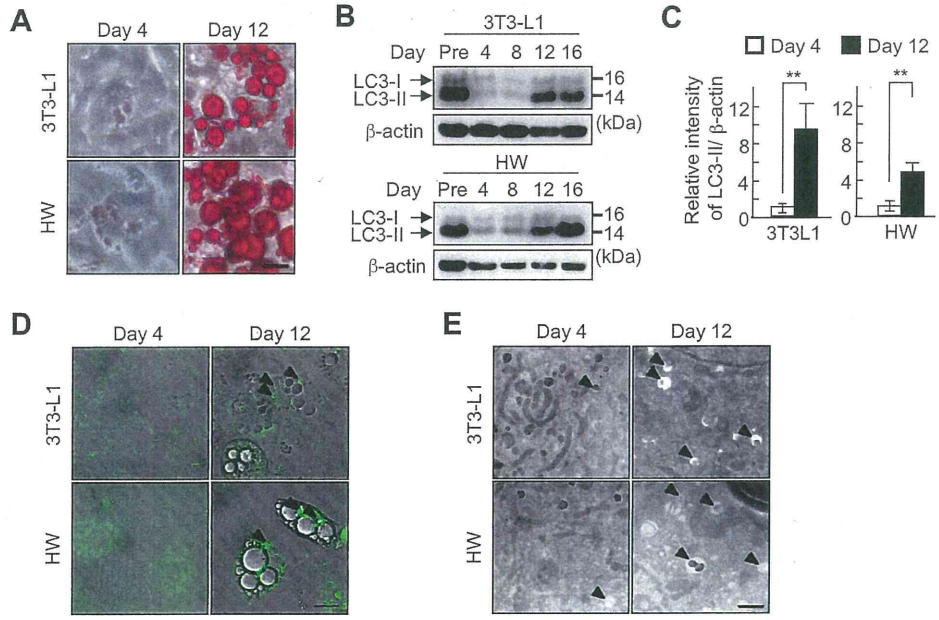

Fig. 2. Autophagy is induced in differentiated and hypertrophic 3T3-L1 and HW adipocytes. (A) Days 4 and 12 3T3-L1 and HW adipocytes were stained with Oil Red O. Scale bar 20 μm. (B) Differentiated adipocytes at the indicated time points were harvested and immunoblot analysis was performed with anti-LC3 and anti-β-actin antibodies. β-Actin was used as a loading control. (C) The results are expressed as the relative intensity of LC3-II/β-actin in day 12 hypertrophic adipocytes compared with day 4 adipocytes. Values are mean ± S.D. (experiments were performed in duplicate with three independent cultures per experiment). Differences between values were analyzed by Student's *t*-test. $^{*}p < 0.05$, $^{**}p < 0.01$. Immunofluorescence analysis with anti-LC3 antibody (D) and electron microscopy analysis (E) were performed at the indicated time points. The arrowheads point at autophagosomes and/or autolysosomes. Scale bars 20 μm and 1 μm, respectively.

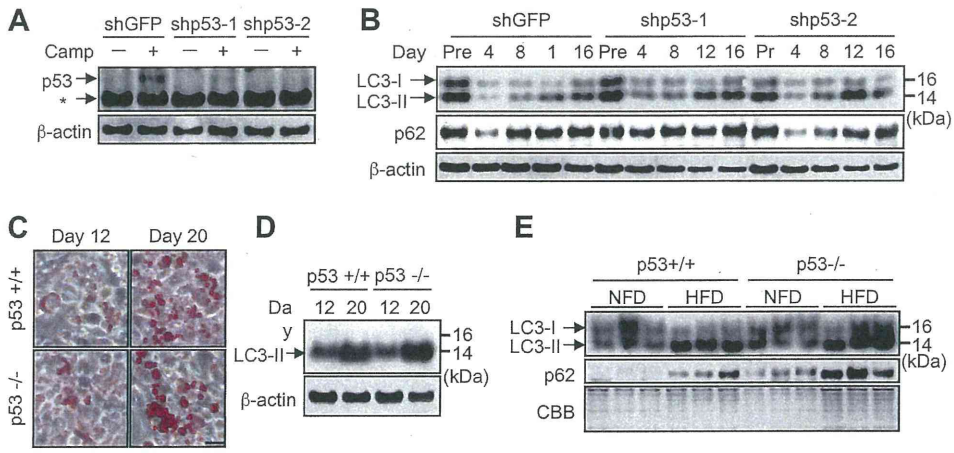

Fig. 3. p53 does not influence autophagy observed in hypertrophic adipocytes and white adipose tissue (WAT) from obese mice. (A) 3T3-L1/shGFP preadipocytes and 3T3-L1/shp53 preadipocytes were treated with 5 μM camptothecin (Camp) for 24 h. Cells were lysed and immunoblot analysis was performed using anti-p53 and anti-β-actin antibodies. β-Actin was used as a loading control. The asterisk indicates nonspecific bands. (B) The differentiated 3T3-L1/shGFP and 3T3-L1/shp53 adipocytes were harvested at the indicated time points and immunoblot analysis was performed with anti-LC3, anti-p62 and anti-β-actin antibodies. β-Actin was used as a loading control. (C, D) Differentiated $p53^{+/+}$ and $p53^{-/-}$ MEFs were stained with Oil Red O staining (C; scale bar 25 μm), or harvested at the indicated time points for immunoblot analysis with anti-LC3 antibody (D). β-Actin was used as a loading control. (E) Representative western blot of LC3. Total protein was extracted from WAT of $p53^{+/+}$ and $p53^{-/-}$ mice fed a normal-fat diet (NFD) or a high-fat diet (HFD) and immunoblot analysis was performed with anti-LC3 and anti-p62 antibodies. CBB stain was used as a loading control. The experiments were performed with 5–6 mice in each group.

To investigate whether p53 influences obesity-induced autophagy *in vivo* as well as *in vitro*, we analyzed the epididymal WAT of wild type ($p53^{+/+}$) and p53-knockout ($p53^{-/-}$) mice, which were fed an NFD or a HFD. HFD increased the body and adipose tissue weight in both mice (data not shown). Previously, it has been reported that obesity increases the expression of p53 in WAT [24,25]. In accordance with these reports, we observed that HFD-induced obesity enhanced p53 expression (data not shown). The conversion of LC3-I to LC3-II and p62 expression were dramatically and equally increased by HFD in both $p53^{+/+}$ and $p53^{-/-}$ mice (Fig. 3E), suggesting that obesity-induced autophagy in mice is regulated in a p53-independent manner as well.

3.3. Autophagic flux is suppressed in differentiated and hypertrophic adipocytes

To clarify whether the autophagic machinery is fully activated in differentiated and hypertrophic adipocytes, we compared

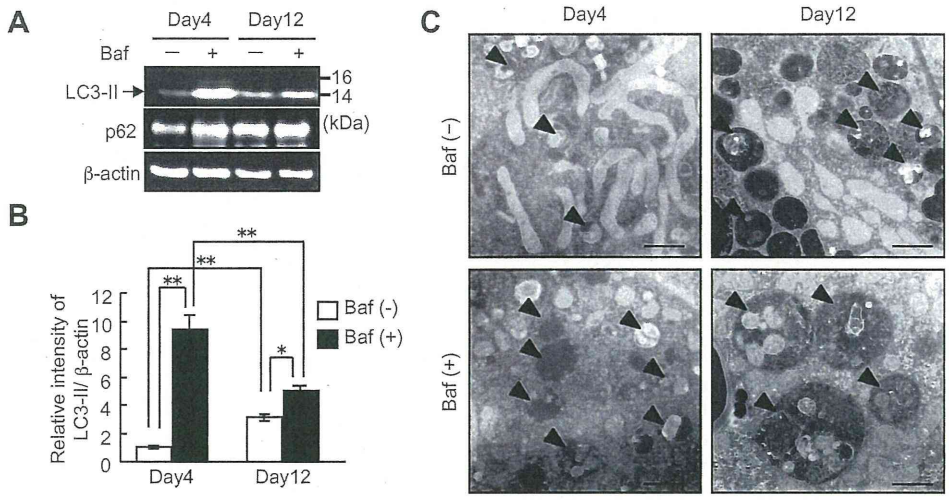

Fig. 4. Autophagic flux is suppressed in differentiated and hypertrophic adipocytes. Day 3 adipocytes and day 11 hypertrophic adipocytes were treated with 10 nM bafilomycin A1 (Baf) for 24 h. (A) Day 4 adipocytes and day 12 hypertrophic adipocytes were harvested and immunoblot analysis was performed with anti-LC3, anti-p62 and anti-β-actin antibodies. β-Actin was used as a loading control. (B) The results are expressed as the relative intensity of LC3-II/β-actin. Values are mean ± S.D. (experiments were performed in duplicate with three independent cultures per experiment). Differences between values were analyzed by Tukey–Kramer test. $^{*}p < 0.05$, $^{**}p < 0.01$. (C) Electron microscopy analysis. The arrowheads point at autophagosomes and/or autolysosomes. Scale bar 1 μm.

autophagic flux of day 12 hypertrophic 3T3-L1 adipocytes with that of day 4 3T3-L1 adipocytes. Treatment with the lysosomal inhibitor, bafilomycin A1 (Baf), significantly increased the expression of LC3-II and p62 in both day 4 adipocytes and day 12 hypertrophic adipocytes (Fig. 4A and B). Unexpectedly, however, the Baf-induced enhancement of the LC3-I to LC3-II conversion and p62 accumulation were lower in day 12 hypertrophic adipocytes than in day 4 adipocytes, suggesting that the autophagic flux was markedly suppressed in day 12 hypertrophic adipocytes compared with day 4 adipocytes (Fig. 4A and B). Using electron microscopy we observed that without Baf treatment day 12 hypertrophic adipocytes contained slightly more autophagosomes than day 4 adipocytes. The autophagosomes' size in day 12 hypertrophic adipocytes was much larger than in day 4 adipocytes (Fig. 4C). After Baf treatment, the autophagosomes' size was markedly increased in both day 4 adipocytes and day 12 hypertrophic adipocytes. Furthermore, regardless of Baf treatment, the autophagosomes containing unspecified structures, which could be undigested contents, were more frequently observed in day 12 hypertrophic adipocytes compared with day 4 adipocytes. Interestingly, unspecified structures were detected in most autophagosomes observed in day 12 hypertrophic adipocytes after Baf treatment (Fig. 4C).

4. Discussion

Previously, it has been reported that p53 is necessary for starvation-induced autophagy in MEFs, HCT116 and Saos-2 cells [7–10]. Herein, we demonstrated that p53 is necessary for starvation-induced autophagy in adipocyte cell lines (3T3-L1 and HW) as well. Electron microscopy analysis revealed that the number of autophagic vacuoles is increased in differentiated and hypertrophic 3T3-L1 adipocytes [11]. However, it has not been clarified yet whether p53 is also required for the autophagy observed in the late stage of adipocyte differentiation. Because differentiated and hypertrophic adipocytes, which accumulate large amounts of TG, may be under stress, we hypothesized that p53 is required for the autophagy observed in differentiated and hypertrophic adipocytes *in vitro* and *in vivo*. Unexpectedly, however, our findings suggest that autophagy observed in differentiated and hypertrophic adipocytes is p53-independent.

Here, we also evaluated the autophagic flux of day 4 adipocytes and day 12 hypertrophic adipocytes, and found that it was markedly suppressed in day 12 hypertrophic adipocytes compared with day 4 adipocytes (Fig. 4A and B). The autophagic machinery consists of three major steps, autophagosome formation, autolysosome formation and degradation of autolysosome contents. During the autolysosome formation, the autophagosome fuses with a lysosome containing many hydrolases. Lieberman et al. [26] hypothesized that lysosomal dysfunction could be seen primarily as autophagy disorder in several types of lysosomal storage diseases. Our electron microscopy analysis of day 12 hypertrophic adipocytes clearly indicated that the autophagosome increases in size and certain structures remain undigested in the autophagosome, and that Baf-treatment enhances the hypertrophy-associated changes. Based on the above-mentioned hypothesis, our data suggest that either autolysosome formation or lysosome function may be impaired in differentiated and hypertrophic adipocytes. Recently, using GFP-LC3 transgenic mice with the lysosome inhibitor, chloroquine, it has been shown that autophagy is suppressed in obese WAT. Moreover, autophagy regulates the inflammatory response in hypertrophic adipocytes [27]. Therefore, we suggest the possibility that autolysosome formation and/or lysosome functions may be impaired in hypertrophic adipocytes *in vitro* and *in vivo*, and the autophagic machinery may be a novel therapeutic target for adipocyte inflammation in obesity and type 2 diabetes.

Acknowledgments

We thank all members of the Molecular Pathology and Metabolic Disease, Animal Center of the Faculty of Pharmaceutical Sciences, Tokyo University of Science, for their cooperation. We thank Dr. Miyoko Irie and Professor Ken Takeda in Hygienic Chemistry, Faculty of Pharmaceutical Sciences, Tokyo University of Science, for their invaluable technical assistance. We also thank Professor Shigeomi Shimizu from Tokyo Medical and Dental University for his helpful suggestions. This work was partially supported by Kyorin Pharmaceutical Co., Ltd.

References

[1] B. Levine, G. Kroemer, Autophagy in the pathogenesis of disease, Cell 132 (2008) 27–42.

[2] I. Tanida, N. Minematsu-Ikeguchi, T. Ueno, E. Kominami, Lysosomal turnover, but not a cellular level, of endogenous LC3 is a marker for autophagy, Autophagy 1 (2005) 84–91.
[3] N. Mizushima, D.J. Klionsky, Protein turnover via autophagy: implications for metabolism, Annu. Rev. Nutr. 27 (2007) 19–40.
[4] N. Mizushima, T. Yoshimori, B. Levine, Methods in mammalian autophagy research, Cell 140 (2010) 313–326.
[5] B. Vogelstein, D. Lane, A.J. Levine, Surfing the p53 network, Nature 408 (2000) 307–310.
[6] S. Matoba, J.G. Kang, W.D. Patino, A. Wragg, M. Boehm, O. Gavrilova, P.J. Hurley, F. Bunz, P.M. Hwang, p53 regulates mitochondrial respiration, Science 312 (2006) 1650–1653.
[7] D.R. Green, J.E. Chipuk, P53 and metabolism: inside the TIGAR, Cell 126 (2006) 30–32.
[8] Z. Feng, H. Zhang, A.J. Levine, S. Jin, The coordinate regulation of the p53 and mTOR pathways in cells, Proc. Natl. Acad. Sci. USA 7 (2005) 8204–8209.
[9] M.C. Maiuri, S.A. Malik, E. Morselli, O. Kepp, A. Criollo, P. Mouchel, R. Carnuccio, G. Kroemer, Stimulation of autophagy by the p53 target gene Sestrin2, Cell Cycle 8 (2009) 1571–1576.
[10] D. Crighton, S. Wilkinson, J. O'Prey, N. Syed, P. Smith, P.R. Harrison, M. Gasco, O. Garrone, T. Crook, K.M. Ryan, DRAM, a p53-induced modulator of autophagy, is critical for apoptosis, Cell 126 (2006) 121–134.
[11] A.B. Novikoff, P.M. Novikoff, O.M. Rosen, C.S. Rubin, Organelle relationships in cultured 3T3-L1 preadipocytes, J. Cell Biol. 87 (1980) 180–196.
[12] R. Baerga, Y. Zhang, P. Chen, S. Goldman, S. Jin, Targeted deletion of autophagy-related 5 (atg5) impairs adipogenesis in a cellular model and in mice, Autophagy 5 (2009) 1118–1130.
[13] R. Singh, Y. Xiang, Y. Wang, K. Baikati, A.M. Cuervo, Y.K. Luu, Y. Tang, J.E. Pessin, G.J. Schwartz, M.J. Czaja, Autophagy regulates adipose mass and differentiation in mice, J. Clin. Invest. 119 (2009) 3329–3339.
[14] Y. Zhanga, S. Goldmana, R. Baergaa, Y. Zhaoa, M. Komatsub, S. Jina, Adipose-specific deletion of autophagy-related gene 7 (atg7) in mice reveals a role in adipogenesis, Proc. Natl. Acad. Sci. USA 106 (2009) 19860–19865.
[15] S. Goldman, Y. Zhang, S. Jin, Autophagy and adipogenesis Implications in obesity and type II diabetes, Autophagy 6 (2010) 179–181.
[16] R. Singh, S. Kaushik, Y. Wang, Y. Xiang, I. Novak, M. Komatsu, K. Tanaka, A.M. Cuervo, M.J. Czaja, Autophagy regulates lipid metabolism, Nature 458 (2009) 1131–1135.
[17] S. Matsushima, N. Okita, M. Oku, W. Nagai, M. Kobayashi, Y. Higami, An Mdm2 antagonist, Nutlin-3a, induces p53-dependent and proteasome-mediated poly(ADP-ribose) polymerase1 degradation in mouse fibroblasts, Biochem. Biophys. Res. Commun. 407 (2011) 557–561.
[18] T. Kamura, T. Hara, M. Matsumoto, N. Ishida, F. Okumura, S. Hatakeyama, M. Yoshida, K. Nakayama, K.I. Nakayama, Cytoplasmic ubiquitin ligase KPC regulates proteolysis of p27Kip1 at G1 phase, Nat. Cell Biol. 6 (2004) 1229–1235.
[19] A.M. Dirac, R. Bernards, Reversal of senescence in mouse fibroblasts through lentiviral suppression of p53, J. Biol. Chem. 278 (2003) 11731–11734.
[20] S. Morita, T. Kojima, T. Kitamura, Plat-E: an efficient and stable system for transient packaging of retroviruses, Gene Ther. 7 (2000) 1063–1066.
[21] N. Nishino, Y. Tamori, S. Tateya, T. Kawaguchi, T. Shibakusa, W. Mizunoya, K. Inoue, R. Kitazawa, S. Kitazawa, Y. Matsuki, R. Hiramatsu, S. Masubuchi, A. Omachi, K. Kimura, M. Saito, T. Amo, S. Ohta, T. Yamaguchi, T. Osumi, J. Cheng, T. Fujimoto, H. Nakao, K. Nakao, A. Aiba, H. Okamura, T. Fushiki, M. Kasuga, FSP27 contributes to efficient energy storage in murine white adipocytes by promoting the formation of unilocular lipid droplets, J. Clin. Invest. 118 (2008) 2808–2821.
[22] C.H. Jung, S. Ro, J. Cao, N.M. Otto, D. Kim, mTOR regulation of autophagy, FEBS Lett. 584 (2010) 1287–1295.
[23] R. Scherz-Shouval, H. Weidberg, C. Gonen, S. Wilder, Z. Elazar, M. Oren, p53-Dependent regulation of autophagy protein LC3 supports cancer cell survival under prolonged starvation, Proc. Natl. Acad. Sci. USA 107 (2010) 18511–18516.
[24] N. Yahagi, H. Shimano, T. Matsuzaka, Y. Najima, M. Sekiya, Y. Nakagawa, T. Ide, S. Tomita, H. Okazaki, Y. Tamura, Y. Iizuka, K. Ohashi, T. Gotoda, R. Nagai, S. Kimura, S. Ishibashi, J. Osuga, N. Yamada, p53 activation in adipocytes of obese mice, J. Biol. Chem. 278 (2003) 25395–25400.
[25] S. Furukawa, T. Fujita, M. Shimabukuro, M. Iwaki, Y. Yamada, Y. Nakajima, O. Nakayama, M. Makisima, M. Matsuda, I. Sgimomura, Increased oxidative stress in obesity and its impact on metabolic syndrome, J. Clin. Invest. 114 (2004) 1752–1761.
[26] A.P. Lieberman, R. Puertollano, N. Raben, S. Slaugenhaupt, S.U. Walkley, A. Ballabio, Autophagy in lysosomal storage disorders, Autophagy 8 (2012) 719–730.
[27] T. Yoshizaki, C. Kusunoki, M. Kondo, M. Yasuda, S. Kume, K. Morino, O. Sekine, S. Ugi, T. Uzu, Y. Nishio, A. Kashiwagi, H. Maegawa, Autophagy regulates inflammation in adipocytes, Biochem. Biophys. Res. Commun. 417 (2012) 352–357.

International Journal of Nephrology and Renovascular Disease Dove

ORIGINAL RESEARCH

Renoprotective effects of telmisartan after unilateral renal ablation in rats

Tomohiro Matsuo
Yasuyoshi Miyata
Yuji Sagara
Yoshikazu Higami
Shohei Tobu
Manabu Matsuo
Mitsuru Noguchi
Isao Shimokawa
Hiroshi Kanetake
Hideki Sakai

Department of Nephro-Urology, Department of Investigative Pathology, Nagasaki University Graduate School of Biomedical Sciences, Nagasaki, Japan

Purpose: The renoprotective function of the angiotensin II type 1 receptor blocker (ARB) is well-known in various studies, including the animal model of renal failure. However, detailed temporal changes of pathological and molecular findings after unilateral nephrectomy are not fully understood. The main purpose of this study was to clarify the renoprotective effects and pathological changes induced by the ARB in rat-remnant kidney (RK) tissues after unilateral nephrectomy, but not after a 5/6 nephrectomy.

Methods: Telmisartan, which is structurally and functionally unique among ARB, was used in this study. Three rat groups were examined: A) no ARB administrated (RK, n=21); B) continuous subcutaneous infusion of an ARB administrated (RK-ARB, n=21); and C) a sham-operated group (Sham). Renal function was evaluated by blood urea nitrogen (BUN) levels and creatinine clearance (Ccr). Fibrosis was evaluated by hydroxyproline levels and Masson's trichrome staining. Expressions of angiotensin II type 1 receptor (AT1R) and transforming growth factor beta (TGF-β) were investigated by real-time polymerase chain reaction and Western blotting.

Results: There was no significant difference regarding body and kidney weight or pathological features evaluated by hematoxylin and eosin staining between the RK and RK-ARB groups. The Ccr in the RK group was significantly lower than that in the Sham group ($P<0.01$), but no significant difference was found between the RK-ARB and Sham groups. The fibrotic area increased significantly with time after nephrectomy in the RK group. Although a similar trend was found in the RK-ARB group, the percentage of fibrous area in the RK-ARB group was significantly lower than that in the RK group at each time point ($P<0.01$). AT1R mRNA levels in the RK group were regulated immediately compared with those in the RK-ARB group. Although expressions of the AT1R and TGF-β were significantly higher in the RK-ARB group than in the Sham group, no significant differences were found between the RK-ARB and Sham group.

Conclusion: The ARB had renoprotective effects after unilateral nephrectomy. The ARB effectively maintained Ccr. Our results also showed the possibility that fibrotic changes mediated by AT1R and TGF-β play an important role in renal protection. Moreover, this is the first report on changes of AT1R expression after using the ARB telmisartan in kidney tissues after unilateral nephrectomy. Finally, our results suggest that ARB may be useful to prevent renal failure in patients treated with nephrectomy.

Keywords: unilateral nephrectomy, telmisartan, angiotensin II type 1 receptor, renoprotection, fibrosis

Correspondence: Yasuyoshi Miyata
Department of Nephro-Urology, Nagasaki University School of Biomedical Sciences, 1-7-1 Sakamoto, Nagasaki 852-8501, Japan
Tel +81 95 819 7340
Fax +81 95 819 7343
Email int.doc.miya@m3.dion.ne.jp

Introduction

Radical nephrectomy is the gold-standard treatment for renal cell carcinoma (RCC). In addition, nephroureterectomy is the standard surgery of urothelial cancer of the

upper urinary tract (UC-UUT). These urological cancers appear commonly in elderly individuals who often have renal dysfunction. Although partial nephrectomy is increasing to avoid renal dysfunction in patients with RCC, it is limited to small RCC. Furthermore, partial resection is not common for patients with UC-UUT. Thus, it is particularly important to preserve remnant kidney function after such unilateral nephrectomy. In addition to patients with RCC and UC-UUT, the preservation of unilateral kidney function is important in the living kidney donor population.[1]

There is general agreement that the renin–angiotensin system (RAS) helps to control blood pressure. In addition, the RAS plays important roles during the initiation and progression of various organ dysfunctions.[2,3] In fact, the RAS inhibition has been shown to have a renoprotective effect, independent of blood pressure.[4,5] Among the components of RAS, angiotensin II has been reported to be associated with renal function through its regulation of several physiological activities, such as the vasomotor tone, glomerular filtration, and accumulation of the extracellular matrix proteins; it also contributes to the progression of tissue inflammation.[6,7,8] In addition, RAS also plays an important role in irreversible organ failure, including that of kidney, due to fibrosis.[8] Thus, understanding the relationship between RAS and the molecular mechanism of fibrosis in kidney tissues is essential to determine the potential preventive strategies for renal function under pathological conditions.

Angiotensin II can reach all accessible target organs to exert its biological and pathological effects by activating its receptors, ie, the angiotensin II type 1 receptors (AT1R) and the angiotensin II type 2 receptors (AT2R). Although the function of AT2R is not fully understood, many studies have shown that the pathophysiological effects of tissues are mainly mediated via binding to AT1R.[9] In fact, AT1R blockade ARB was found to be effective not only for lowering blood pressure, but it was also found to be effective in protecting against remodeling and functionally preserving the kidney.[10] In addition, clinical evidence has demonstrated that ARB could improve renal function or slow disease progression in nephropathy.[11] Thus, information regarding the relationship between ARB and AT1R is important to understand the detailed mechanisms involved in this renoprotective effect.

Many reports have been published regarding the relationship between ARBs and their renoprotective function in vivo. However, most reports have focused on the chronic kidney disease that occurs with hypertension and diabetes mellitus. On the other hand, several reports have shown the renoprotective effects of ARBs and/or AT1Rs in acute renal failure by using a subtotal of nephrectomized animal models.[12,13] However, this situation is not common under clinical conditions. Conversely, despite the fact that unilateral nephrectomy is the standard surgery for a variety of urological cancers and transplantation, there is little detailed information on the renoprotective mechanisms of ARB in such pathological conditions in vivo.

The purpose of this study was to clarify the renoprotective effects of ARB after the unilateral nephrectomy in animal models that fit into the reality of clinical situations. In addition, changes of the AT1R mRNA and protein expression were investigated in a similar model. We also examined the relationship between the AT1 expression and hydroxyproline (Hyp), a fibrotic marker, and transforming growth factor beta (TGF-β), a representative renal fibrosis-related molecule, in unilateral nephrectomized rat kidney tissues treated with ARB.

Methods

Animal models

Twelve-week-old male F344 rats (n=70; Charles River Laboratories, Inc, Yokohama, Japan) were used. Under pentobarbital sodium anesthesia (50 mg/kg intraperitoneally), the left kidney was removed. The removed kidney was dissected and prepared for histology, immunohistochemical study, Western blotting, and a real-time reverse transcription–polymerase chain reaction (RT–PCR). Samples for Western blotting and RT–PCR were snap-frozen in liquid nitrogen and stored at −80°C. The muscle and skin layers were closed after subcutaneous implantation of osmotic minipumps (Alzet model 2004, DURECT Corporation, Cupertino, CA, USA) filled with dimethyl sulfoxide or telmisartan (Nippon Boehringer Ingelheim Co, Ltd, Tokyo, Japan).

Twenty-one rats underwent anesthesia and manipulation of the renal pedicles without removal of any renal mass (Sham group). These rats were housed in individual cages in a temperature-controlled room at 22°C and a 12-hour light/dark cycle (Laboratory Animal Center for Biomedical Research, Nagasaki University School of Medicine, Nagasaki, Japan), fed a standard diet, and allowed to drink tap water ad libitum. All procedures were performed according to the protocols approved by the Animal Care and Use Committee of Nagasaki University.

Experimental rat groups

A total of 42 nephrectomized rats were divided into two groups: the A) renal ablation group treated with physiological